

# Nickel-Doped TiO<sub>2</sub> Multilayer Thin Film for Enhancement of Photocatalytic Activity

Yoshiki Kurokawa, Dang Trang Nguyen, Kozo Taguchi\*

Department of Science and Engineering, Ritsumeikan University, 1-1-1 Noji Higashi, Kusatsu, Shiga, 525-8577, Japan.

\* Corresponding author. Tel.: +81-77-561-5178; email: taguchi@se.ritsumei.ac.jp

Manuscript submitted November 25, 2018; accepted February 1, 2019.

doi: 10.17706/ijmse.2019.7.1.10-19.

---

**Abstract:** The nickel-doped titanium powder and multilayer thin films for photocatalytic experiment were investigated. In order to improve the photocatalytic activity of TiO<sub>2</sub> in the visible region, nickel-doped TiO<sub>2</sub> powder was fabricated by Sol-Gel method. Moreover, we also studied the relationship between thin film surface conditions and photocatalytic activity. Based on experimental results, nickel-doped TiO<sub>2</sub> powder absorbed slightly visible light, and multilayer thin films reduced cracks on the surface. Multilayer thin films made of commercial P25 TiO<sub>2</sub> powder mixed with nickel-doped powder enabled the highest photocatalytic activity.

**Key words:** Electrophoresis deposition, multilayer thin film, Ni-doped TiO<sub>2</sub> powder, photocatalyst.

---

## 1. Introduction

In textile and other industries, wastewater has been produced in the process of dyeing products. They contain dangerous organic compounds which affect negatively to the environment. Due to such serious problems, removing dangerous organic compounds from wastewater is required. There are some methods that can remove dangerous organic compounds. Among them, photocatalyst technology has attracted attention in recent years [1]–[5].

A photocatalyst is a material that causes chemical reaction using light energy, and it is used in some applications, for example, medical facilities, automobile mirrors and air conditioners deodorant filters. It is also used for organic matter degradation and expected to solve this environmental problem. The working principle of the photocatalytic organic-matter-degradation reaction is as follows; first, photocatalytic materials absorb light that contains higher energy than the band gaps of the materials. Then electrons (e<sup>-</sup>) transfer from the valence band (VB) to the conduction band (CB) of the photocatalytic materials. Positive holes (h<sup>+</sup>), which are electron-lack, are created at the VB. Positive holes deprive electrons of the (OH) group in water on the photocatalyst surfaces. (OH) group deprived electrons (OH radical) is in unstable condition, it deprives electrons from nearby organic matters. Then, it becomes stable. Electrons in CB reduce oxygen in the air, and superoxide anion (O<sub>2</sub><sup>-</sup>) is created. The OH radical and O<sub>2</sub><sup>-</sup> are called active oxygen and they have strong oxidizing power. They attack organic matters present near the surfaces of the photocatalytic materials. Ultimately, this process causes complete degradation of organic matters into harmless molecules as shown in Fig. 1 [6]–[8]. As photocatalytic materials TiO<sub>2</sub>, CdS, Fe<sub>2</sub>O<sub>3</sub>, WO<sub>3</sub>, and ZnO are well-known.

Among them, anatase  $\text{TiO}_2$  is widely used as a photocatalytic material due to its optical and electronic properties of high stability, low cost, and non-toxicity [6], [7], [9], [10]. Because this material has wide band gap (3.2 eV) which can respond to only a small fraction of the solar spectrum (<380 nm wavelength, UV light) [10]–[13]. Sunlight spectrum only contains about 5 % UV light. Therefore, many researchers have been trying to extend the response of  $\text{TiO}_2$  to visible light (400~800 nm wavelength) by using the method of doping some metals in  $\text{TiO}_2$ . Doping non-noble metals (Fe, Ni, Cu) to  $\text{TiO}_2$  is more practical, which has been used to decrease the band gap of  $\text{TiO}_2$  and to extend the photo-response range of  $\text{TiO}_2$  to the visible light region [14]. Ni has some characteristics, such as resistance to corrosion and oxidation, easy to alloy, coverable by electroplating, catalyst characteristics. Ni can reduce band gap and attribute to the suppression of the recombination of electron-hole pairs on the  $\text{TiO}_2$  surface [7], [9], [11], [12], [15]–[19].

In this study, we tried to fabricate smooth, multilayer, Ni-doped  $\text{TiO}_2$  thin films for improving photocatalytic activity. Thin film catalyst is more practical than powder catalyst because of its simple reusability. The quality of thin film surface is an important factor. In the process of making thin film, cracks on the surface occurred because of the evaporation of the solvent as shown in Fig. 2 [20], [21]. To our knowledge, there has been no study that reported on the relationship between the quality of  $\text{TiO}_2$  thin film and its photocatalytic activity. We attempted to reduce cracks by making multilayer thin film. Ni-doped  $\text{TiO}_2$  powder was fabricated by Sol-Gel method to extend the optical absorption band of  $\text{TiO}_2$  to visible range.

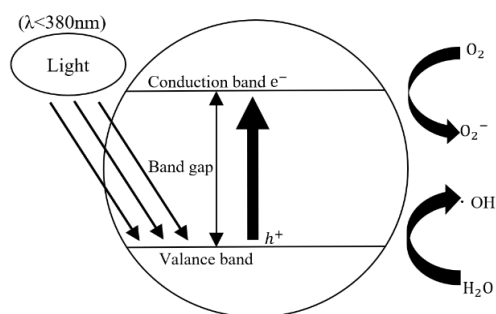


Fig. 1. Photocatalyst theory.

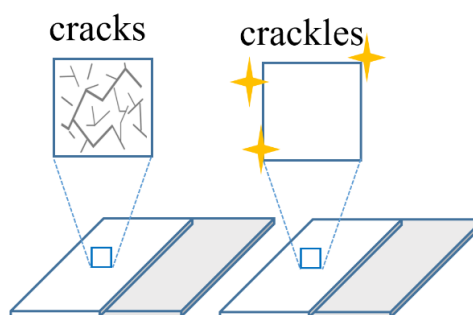


Fig. 2. Cracks on thin film.

## 2. Method

### 2.1. Sol-Gel method

To make Ni-doped  $\text{TiO}_2$  powder by Sol-Gel method, we mixed 6 ml of Titanium Tetraisopropoxide (TTIP), 20mL of ethanol, 1mL of deionized water and 0.01mol of  $(\text{Ni}(\text{NO}_3)_2 \cdot 6\text{H}_2\text{O})$  in a container using a magnetic stirrer rotating at the speed of 500rpm for 1 hour. Then, the prepared solution was dried at  $100^\circ\text{C}$  for about 3 hours. After that, the obtained dried gel was grinded in a mortar to become fine powder. The powder was annealed at  $650^\circ\text{C}$  for 1 hour for crystallizing. The completed Ni-doped  $\text{TiO}_2$  powder was called as Ni-SP.

Table 1. EPD Solution Materials

sample	Powder	Ethanol
P25	P25 0.1g	20mL
P25+Ni SP	P25 0.1g, Ni SP 0.02g	20mL

### 2.2. EPD

To make thin films, we adopted electrophoresis deposition method (EPD). EPD is a method which charged minute particles in solvent by applying external electric field and deposited them on an electrode

substrate. In this method, thin film with controllable thickness can be produced. EPD charges  $\text{TiO}_2$  particles in EPD solution positively and so they move to the negative charged electrode [21]–[24]. Commercially available  $\text{TiO}_2$  powder (P25, particle size: 20nm) without or with Ni-SP powder was mixed with ethanol as shown in Table 1. They are mixed at the speed of 700rpm for 1 hour with a magnetic stirrer. The anode (aluminum plate,  $20 \times 20 \times 1\text{mm}$ ) and cathode (FTO glass,  $20 \times 20 \times 1.8\text{mm}$ ) were placed 10mm in parallel into the prepared EPD solutions as shown in Fig. 3. EPD current from a current source (ADVANTEST, R6144) was set at 0.12mA and EPD time was 100sec in total. To make multilayer thin film (four layers), we performed 25 seconds EPD four times and respectively drying at  $60^\circ\text{C}$  for 1min three times. The deposited areas were the same ( $10 \times 20\text{mm}$ ). After completing deposition,  $\text{TiO}_2$  thin films were annealed in the air at  $400^\circ\text{C}$  ( $5^\circ\text{C}/\text{min}$  heating rate) for 1 hour with an electric furnace (ASONE SMF-1). Because of the same total EPD time, both single-layer and four-layer thin films had the same thickness of about  $15\mu\text{m}$ .

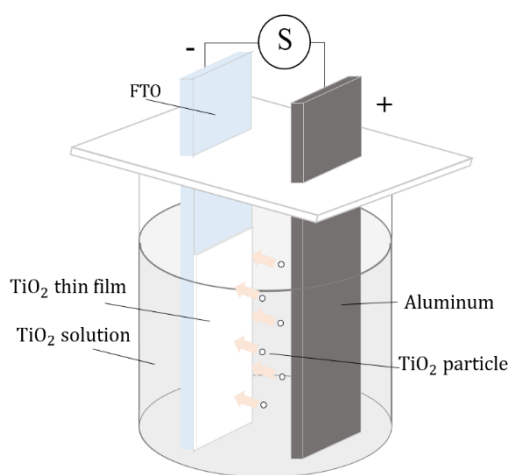


Fig. 3. EPD device.

### 2.3. Powder and Thin Film Characterization Method

A Scanning Electron Microscope (SEM, HITACHI S4300) was used to observe Ni-SP powder, P25 thin films, and P25+Ni-SP thin films.

An X-ray diffraction spectroscopy (XRD, PANalytical) was used to measure crystalline morphology and quantitative analysis of P25, Ni-SP, and P25 + Ni-SP powders.

A UV-vis spectrophotometer (SHIMAZU, UV-3600) was used to evaluate the absorption band of the thin films. The transmittance and reflectance of two types of  $\text{TiO}_2$  thin films (P25 single layer and P25+Ni-SP single layer) were measured to determine their UV-visible spectra.

Four types of  $\text{TiO}_2$  thin films (P25 single layer, P25 four layers, P25+Ni-SP single layer, and P25+Ni-SP four layers) were immersed in methylene blue solution ( $1.0 \times 10^{-4}\text{M}$ ) for three hours in the dark. Then, they were taken out for dry and subsequently measured by the UV-vis spectrophotometer to compare methylene blue absorption rate in these thin films, in other words, to determine the active surface area of these thin films.

### 2.4. Methylene Blue Photocatalytic Degradation Experiment

The photocatalytic activity of the fabricated thin films was evaluated based on their methylene blue degradation rates. methylene blue is a cationic dye used as a traditional dye for dyeing cotton, wool, and silk. This experiment was performed using  $1.0 \times 10^{-5}\text{M}$  methylene blue aqueous dye solution. A UV light source was used (TOSHIBA, FL20S-BL lamp), which illuminates ultraviolet and a narrow band of visible light (400-500nm wavelength). As shown in Fig. 4, transparent plastic containers were filled with 5ml of the

methylene blue solution. The fabricated thin films were immersed into these containers. Then, they were irradiated by the lamp with a 5cm distance from the lamp. Every one-hour interval, 1ml solution was taken out of each container for measuring the transmittance by the UV-vis spectrophotometer. After the measurement, we returned the taken-out solution to the corresponding container for further photocatalytic degradation experiment. We repeated the measurement six times in total. The methylene blue degradation rate is proportional to the absorbance, which is calculated using the following equation (1) [11], [12], [25], [26].

$$\text{Absorbance (abs)} = \ln \left( \frac{T_0}{T_t} \right) \quad (1)$$

(where,  $T_0$ : initial transmittance and  $T_t$ : Transmittance at given time).

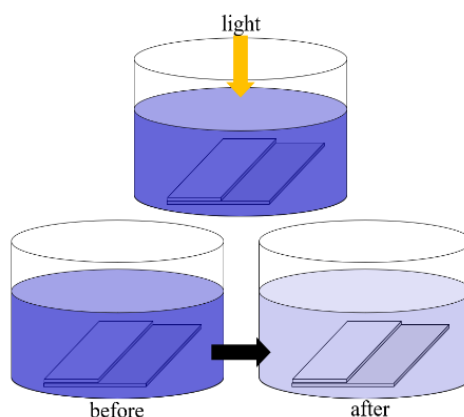


Fig. 4. Experimental setup of the methylene blue photocatalytic degradation experiment.

### 3. Result and Discussion

#### 3.1. Powder and Thin Film Characterization

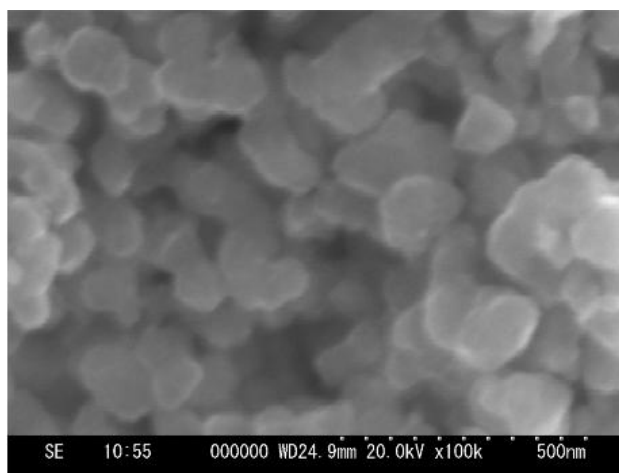


Fig. 5. SEM image of the fabricated Ni-SP powder.

Fig. 5 shows the SEM image of the handmade Ni-SP powder. The particle diameter is about 100nm. Commercially available P25 powder has about 20nm diameter particles, so Ni-SP particles are about 5 times larger than P25 particles. In addition, Fig. 6 shows the SEM images of the fabricated thin films: (a) P25 single layer, (b) P25+Ni-SP single layer, (c) P25 four layers, and (d) P25+Ni-SP four layers. From Fig 6 (a) (b), there were many cracks on the surfaces of these single layer thin films. These cracks caused to

reduce the surface area of these thin films. On the other hand, there was almost no crack observed on the surfaces of the four-layer thin films (Fig. 6 (c) (d)), it can be confirmed that multilayer fabrication method can improve the quality of the thin films and increase their effective surface area.

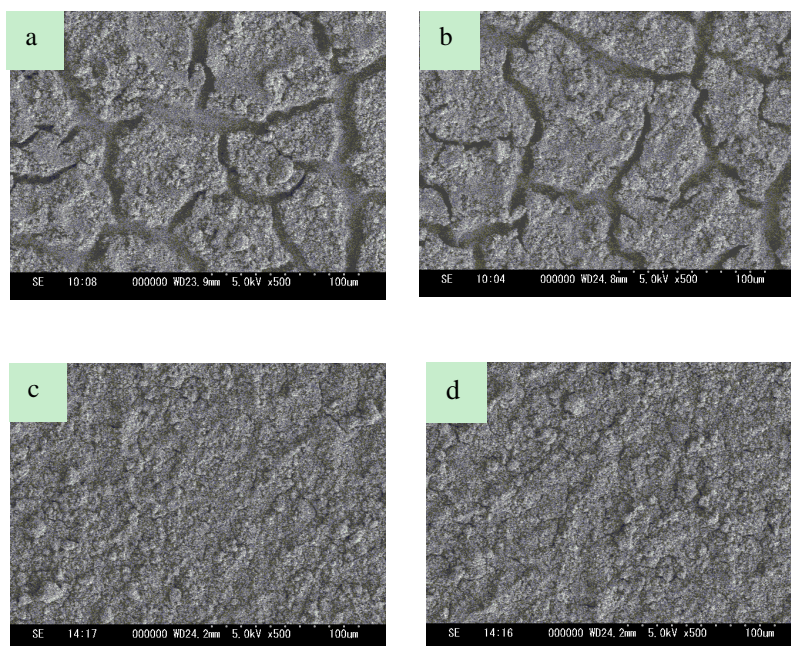


Fig. 6. SEM images of (a) P25 single layer, (b) P25+Ni-SP single layer (c) P25 four layers, (d) P25+Ni-SP four layers.

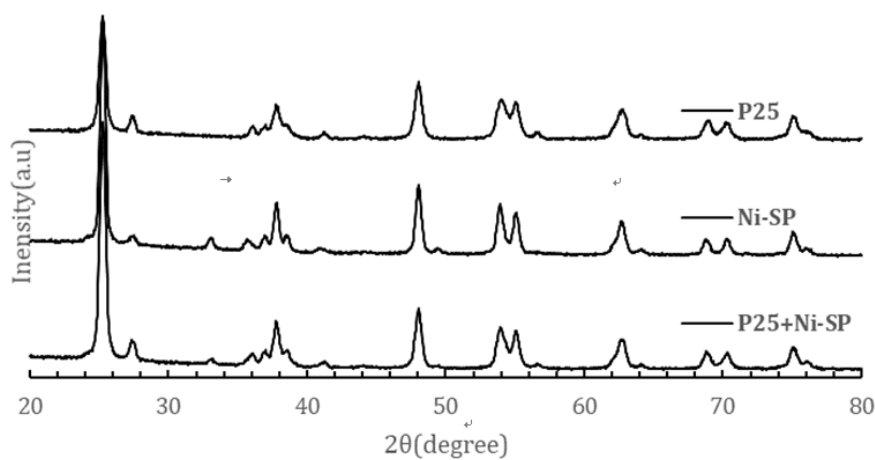


Fig. 7. XRD data.

Fig. 7 shows XRD diffraction pattern of three types of  $\text{TiO}_2$  powder (P25, Ni-SP, P25 + Ni-SP). These powders had strong peaks in anatase and rutile. Anatase peaks recognized at  $25.26^\circ$ ,  $37.74^\circ$ ,  $48.03^\circ$ ,  $53.84^\circ$ ,  $55.06^\circ$ ,  $62.10^\circ$ ,  $68.73^\circ$ ,  $70.31^\circ$ , and  $75.04^\circ$ . Generally, anatase  $\text{TiO}_2$  causes photocatalytic reaction. Furthermore, both Ni-SP and P25+Ni-SP powders had a peak at  $33.13^\circ$  that was absence in P25 powder. That was one of the two peaks of  $\text{TiNiO}_3$  ( $33.13^\circ$  and  $49.48^\circ$ ). Based on the result of quantitative analysis of XRD data, P25 contained 77% of anatase and 23% of rutile; Ni-SP contained 66% of anatase, 16% of rutile, and 18% of  $\text{TiNiO}_3$ ; P25+Ni-SP contained 75% of anatase, 16% of rutile, and 9% of  $\text{TiNiO}_3$ . From these results, it can be inferred that the nickel-doped  $\text{TiO}_2$  was successfully prepared by the sol-gel method.

Fig. 8 shows the UV-vis spectra of the thin films of P25 single layer and P25 + Ni-SP single layer. The light absorption characteristics of the P25 thin film (black solid line) were much decreased after the wavelength

of 400nm. This shows the light absorption characteristics of non-doped  $\text{TiO}_2$ , its response is in the UV light only. P25+Ni-SP thin film (red dotted line) had light absorption characteristics in a faint visible light range (400-470 nm). This is the effect of Ni-doped  $\text{TiO}_2$  prepared by the sol-gel method. It can be confirmed that by using Ni-doped method, we have succeeded in extending the absorption wavelength of  $\text{TiO}_2$ .

Fig. 9 shows the methylene blue absorptivity in  $\text{TiO}_2$  thin films after three hours immersed into methylene blue solution in the dark. Four types of  $\text{TiO}_2$  thin films (P25 single layer, P25 four layers, P25+Ni-SP single layer, and P25+Ni-SP four layers) were measured. The P25+Ni-SP four-layer thin film showed the highest absorptivity, and the P25 single-layer thin film showed the lowest absorptivity. If comparing P25 single-layer and P25 four-layer thin films (black solid line and black dashed line) with P25+Ni-SP single-layer thin film and P25+Ni-SP four-layer thin film (red dotted line and red dashed dotted line), the samples with four layers show higher methylene blue absorptivity in both cases. This result indicates that the surface area of four-layer thin films was significantly improved because of the absence of cracks. Furthermore, there was almost no difference in absorptivity between the P25 four layers and P25+Ni-SP single layer. This is an indication of the effect of Ni-doped powder on the improvement of the thin film surface area.

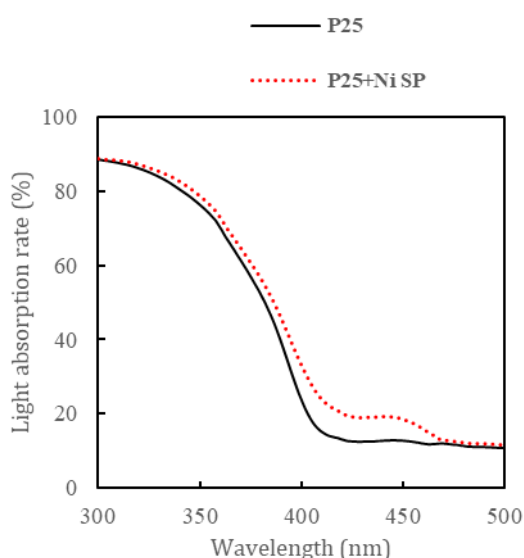


Fig. 8. UV-vis spectra of P25 single-layer and P25+Ni-SP single-layer thin films.

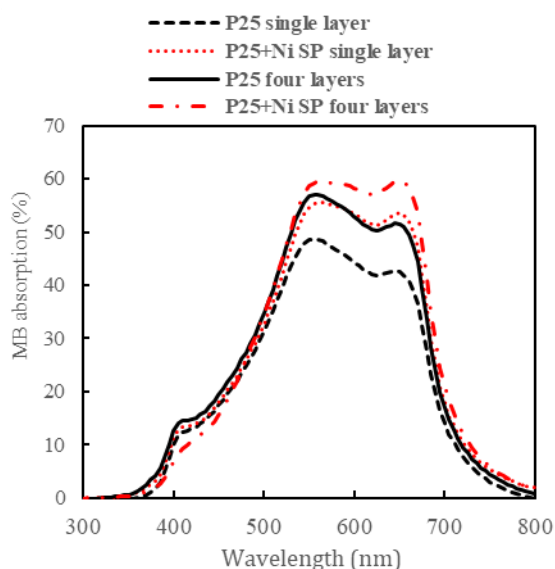


Fig. 9. UV-vis spectra of four methylene blue-absorbed  $\text{TiO}_2$  thin films.

### 3.2. Methylene Blue Photocatalytic Degradation Experiment

Fig. 10 shows the photocatalytic degradation of methylene blue dye by the four thin films of (a) P25 single layer, (b) P25 four layers, (c) P25+Ni-SP single layer, and (d) P25+Ni-SP four layers. The light irradiation time was 6 hours. The absorbance was calculated based on equation (1). A deionized water sample was also measured for comparison (dashed lines in Fig. 10). When the change from the initial absorbance is large, the degradation rate is high. As expected, the P25 single-layer thin film (Fig. 10 (a)) and P25+Ni-SP four-layer thin film (Fig. 10 (d)) had the lowest and highest rates of degradation, respectively.

Fig. 11 shows methylene blue degradation rate as a function of light irradiation time (6 hours). Methylene blue degradation rate was obtained from the ratio of the absorbance at the maximum absorption wavelength (664nm) in Fig. 10. In the same light irradiation period, the P25 + Ni-SP four-layer thin film showed the highest methylene blue degradation rate of 76.1%. Meanwhile, P25 single-layer thin film showed the lowest methylene blue degradation rate of 57.7%. In addition, methylene blue degradation rate of the P25 four-layer thin film was 69.1%, which was similar to 68.7% of the P25 + Ni-SP single-layer thin film. This was attributed

to the positive effect of the fabricated nickel-doped  $\text{TiO}_2$  powder mixed in the P25 + Ni-SP single-layer thin film. In the case of the samples with the same type of powder, cracks on the thin film surfaces were negatively related to their photocatalytic activity. Therefore, the four-layer thin film showed higher methylene blue degradation rate than the single-layer thin film.

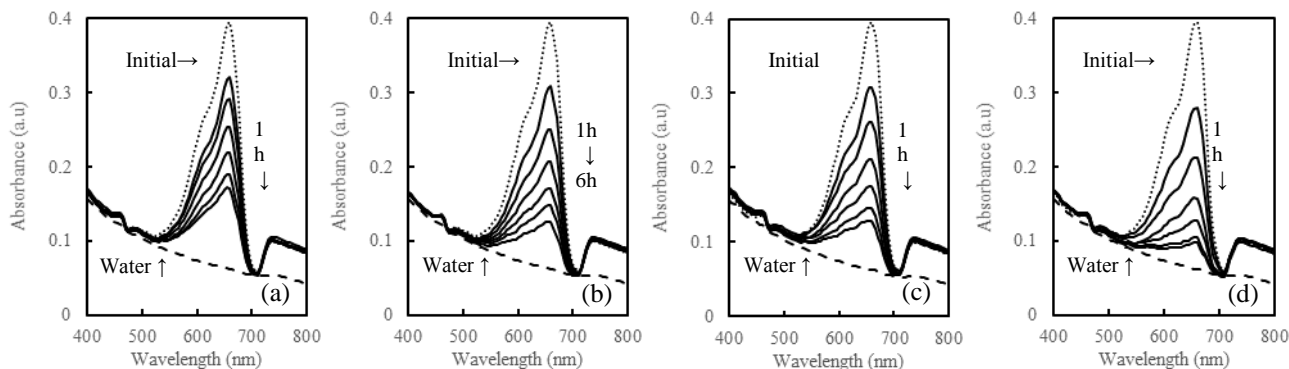


Fig. 10. Photocatalytic degradation of methylene blue dye in the presence of (a) P25 single layer, (b) P25 four layers, (c) P25+Ni-SP single layer, (d) P25+Ni-SP four layers. Dashed lines in all figures represent the absorbance of deionized water sample.

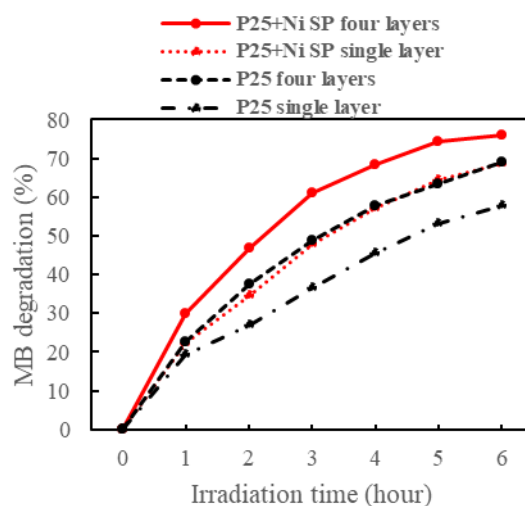


Fig. 11. Photocatalytic degradation rate of methylene blue dye under light irradiation.

#### 4. Conclusions

From the experimental results, we can conclude that P25+Ni-SP multilayer thin film enhances the photocatalytic activity. This is because of the extension of the absorption wavelength of Ni-doped  $\text{TiO}_2$  and the reduction of cracks in the multilayer thin film resulted in larger reaction area. P25+Ni-SP four-layer thin film realized an improvement of 31.8% in methylene blue photocatalytic degradation rate compared with P25 single-layer thin film. In the future, we will optimize the capability of photocatalytic activity of P25+Ni-SP powder by varying the ratio of P25 and Ni-SP powders.

#### Acknowledgment

The authors wish to thank to Minemoto laboratory of Ritsumeikan University. We got to use XRD (PANalytical), step gauge (BRUKER DektakXT) and UV-vis spectrophotometer (SHIMADZU, UV-3600) from Minemoto laboratory.

## References

- [1] Mo, J. H., Lee, Y. H., Kim, J., Jeong, J. Y., & Jegal, J. (2008). Treatment of dye aqueous solutions using nanofiltration polyamide composite membranes for the dye wastewater reuse. *Dyes and Pigments*, 76, 429–434.
- [2] Vadivelan, V., & Vasanth, K. K. (2005). Equilibrium, kinetics, mechanism, and process design for the sorption of methylene blue onto rice husk. *Journal of Colloid and Interface Science*, 286, 90–100.
- [3] Ahmad, A. L., & Puasa, S. W. (2007). Reactive dyes decolourization from an aqueous solution by combined coagulation/micellar-enhanced ultrafiltration process. *Chemical Engineering Journal*, 132, 257–265.
- [4] Choi, H., Antoniou, M. G., de la Cruz, A. A., Stathatos, E., & Dionysiou, D. D. (2007). Photocatalytic TiO<sub>2</sub> films and membranes for the development of efficient wastewater treatment and reuse systems. *Desalination*, 202, 199–206.
- [5] Shimizu, N., Ogino, C., Dadjour, M. F., & Murata, T. (2007). Sonocatalytic degradation of methylene blue with TiO<sub>2</sub> pellets in water. *Ultrasonics Sonochemistry*, 14, 184–190.
- [6] Kerkez-Kuyumcu, Ö., Kibar, E., Dayıoğlu, K., Gedik, F., Akın, A. N., & Özkara-Aydınoglu, Ş. (2015). A comparative study for removal of different dyes over M/TiO<sub>2</sub> (M=Cu, Ni, Co, Fe, Mn and Cr) photocatalysts under visible light irradiation. *Journal of Photochemistry and Photobiology A: Chemistry* 311, 176–185.
- [7] Blanco-Vega, M. P., Guzmán-Mar, J. L., Villanueva-Rodríguez, M., Maya-Treviño, L., Garza-Tovar, L. L., Hernández-Ramírez, A., *et al.* (2017). Photocatalytic elimination of bisphenol A under visible light using Ni-doped TiO<sub>2</sub> synthesized by microwave assisted sol-gel method. *Materials Science in Semiconductor Processing*, 71, 275–282.
- [8] Ghaly, M. Y., Jamil, T. S., El-Seesy, I. E., Souaya, E. R., & Nasr, R. A. (2011). Treatment of highly polluted paper mill wastewater by solar photocatalytic oxidation with synthesized nano TiO<sub>2</sub>. *Chemical Engineering Journal*, 168(1), 446–454.
- [9] Ganesh, I., Gupta, A. K., Kumar, P. P., Sekhar, P. S. C., Radha, K., Padmanabham, G., *et al.* (2012). Preparation and characterization of Ni-doped materials for photocurrent and photocatalytic applications. *The Scientific World Journal*, 2012, 1–16.
- [10] Yang, Y., Xu, L., Wang, H., Wang, W., & Zhang, L. (2016). TiO<sub>2</sub>/graphene porous composite and its photocatalytic degradation of methylene blue. *Materials and Design*, 108, 632–639.
- [11] Fisher, M. B., Keane, D. A., Fernández-Ibáñez, P., Colreavy, J., Hinder, S. J., McGuigan, K. G., *et al.* (2013). Nitrogen and copper doped solar light active TiO<sub>2</sub> photocatalysts for water decontamination. *Applied Catalysis B: Environmental*, 131, 8–13.
- [12] Jagadale, T. C., Takale, S. P., Sonawane, R. S., Joshi, M., Patil, S. I., Kale, B. B., *et al.* (2008). N-Doped TiO<sub>2</sub> nanoparticle based visible light photocatalyst by modified peroxide sol - gel method. *Journal of Physical Chemistry C*, 112, 14595–14602.
- [13] Yoong, L. S., Chong, F. K., & Dutta, B. K. (2009). Development of copper-doped TiO<sub>2</sub> photocatalyst for hydrogen production under visible light. *Energy*, 34, 1652–1661.
- [14] Sonawane, R. S., Kale, B. B., & Dongare, M. K. (2004). Preparation and photo-catalytic activity of Fe-TiO<sub>2</sub> thin films prepared by sol-gel dip coating. *Materials Chemistry and Physics*, 85, 52–57.
- [15] Chen, J., Yao, N., Wang, R., & Zhang, J. (2009). Hydrogenation of chloronitrobenzene to chloroaniline over Ni/TiO<sub>2</sub> catalysts prepared by sol-gel method. *Chemical Engineering Journal*, 148, 164–172.
- [16] Hung, W. C., Fu, S. H., Tseng, J. J., Chu, H., & Ko, T. H. (2007). Study on photocatalytic degradation of gaseous dichloromethane using pure and iron ion-doped TiO<sub>2</sub> prepared by the sol-gel method. *Chemosphere*, 66(11), 2142-2151.

- [17] Yuan, Z., Jia, J., & Zhang, L. (2002). Influence of co-doping of Zn(II)+Fe(III) on the photocatalytic activity of TiO<sub>2</sub> for phenol degradation. *Materials Chemistry and Physics*, 73, 323–326.
- [18] Nakhate, G. G., Nikam, V. S., Kanade, K. G., Arbuj, S., Kale, B. B., & Baeg, J. O. (2010). Hydrothermally derived nanosized Ni-doped TiO<sub>2</sub>: A visible light driven photocatalyst for methylene blue degradation. *Materials Chemistry and Physics*, 124, 976–981.
- [19] Jing, L., Xin, B., Yuan, F., Xue, L., Wang, B., & Fu, H. (2006). Effects of surface oxygen vacancies on photophysical and photochemical processes of Zn-doped TiO<sub>2</sub> nanoparticles and their relationships. *Journal of Physical Chemistry B*, 110, 17860–17865.
- [20] Chang, H., Su, H. T., Chen, W. A., David, H. K., Chien, S. H., Chen, S. L., *et al.* (2010). Fabrication of multilayer TiO<sub>2</sub> thin films for dye-sensitized solar cells with high conversion efficiency by electrophoresis deposition. *Solar Energy*, 84(1), 130–136.
- [21] Ruhane, T. A., Islam, M. T., Rahaman, M. S., Bhuiyan, M. M. H., Islam, J. M. M., Bhuiyan, T. I., *et al.* (2017). Impact of photo electrode thickness and annealing temperature on natural dye sensitized solar cell. *Sustainable Energy Technologies and Assessments*, 20, 72–77.
- [22] Shikoh, A. S., Ahmad, Z., Touati, F., Shakoor, R. A., & Al-Muhtaseb, S. A. (2017). Optimization of ITO glass/TiO<sub>2</sub> based DSSC photo-anodes through electrophoretic deposition and sintering techniques. *Ceramics International*, 43(13), 10540–10545.
- [23] Rama K. C., Lee, W. M., Oh, S. Y., Jeong, K. U., & Yu, Y. T. (2017). Improvement in light harvesting and device performance of dye sensitized solar cells using electrophoretic deposited hollow TiO<sub>2</sub> NPs scattering layer. *Solar Energy Materials and Solar Cells*, 161, 255–262.
- [24] Grinis, L., Dor, S., Ofir, A., & Zaban, A. (2008). Electrophoretic deposition and compression of titania nanoparticle films for dye-sensitized solar cells. *Journal of Photochemistry and Photobiology A: Chemistry*, 198, 52–59.
- [25] Ahmed, M. A. (2012). Synthesis and structural features of mesoporous NiO/TiO<sub>2</sub> nanocomposites prepared by sol-gel method for photodegradation of methylene blue dye. *Journal of Photochemistry and Photobiology A: Chemistry*, 238, 63–70.
- [26] Dariani, R. S., Esmaeili, A., Mortezaali, A., & Dehghanpour, S. (2016). Photocatalytic reaction and degradation of methylene blue on TiO<sub>2</sub> nano-sized particles. *Optik*, 127, 7143–7154.



**Yoshiki Kurokawa** was born in Shiga, Japan on April 26, 1994. He received bachelor's degree in the Department of Science and Engineering from Ritsumeikan University, Shiga, Japan in March 2017 and was admitted to a postgraduate course at same university in April 2017. He also belongs to an electronics system course of Department of Science and Engineering. He is now in the second year. He is making a study of photocatalyst by using electrophoresis deposition in the graduate course.



**D. Trang Nguyen** was born in Vietnam in 1986. He received the BS degree in 2009 from the Department of Telecommunication Systems Hanoi University of Science and Technology, Hanoi, Vietnam. After that he received the ME in 2011 from the Department of Electronics and Electrical Engineering, Dongguk University, Seoul, South Korea. From 2011 to 2014, he completed his Ph.D program in integrated science and engineering at Ritsumeikan University, Kyoto, Japan. After earning his Ph.D, he was a quality assurance engineer at Takako Industries, Inc. from 2015 to 2017. Currently, he is a senior researcher at the Ritsumeikan Global Innovation Research Organization, Ritsumeikan University. His fields of interest include biofuel cells, solar cells, biosensors, and hydrogen energy.



**Kozo Taguchi** was born in Kyoto, Japan, on December 18, 1968. He received the B.E., M.E., and Dr. Eng. degrees in electrical engineering from Ritsumeikan University, Kyoto, Japan, in 1991, 1993, and 1996, respectively. In 1996, he joined Fukuyama University, Hiroshima, Japan, where he had been engaged in research and development on the optical fiber trapping system, semiconductor ring lasers and their application for optoelectronics devices, and polymeric optical waveguides for optical interconnection. In 1996–2003, he worked as an assistant and lecturer in Fukuyama University. In 2003, he moved to Ritsumeikan University, Shiga, Japan, and currently he is a professor of department of electric and electronic engineering. From 2006 to 2007, he was a visiting professor at University of St Andrews (Scotland, United Kingdom). From 2014 to 2015, he was a visiting professor at Nanyang Technological University (Singapore). His current research interests include cells trap, microfluidic cell-based devices, dye sensitized solar cell, biofuel cells, biosensors, and hydrogen energy. Dr. Taguchi is a member of the JJAP.